

## Theory of the phase-transition sequence in betaine calcium chloride dihydrate (BCCD)

Z. Y. Chen\* and M. B. Walker

*Department of Physics, University of Toronto, Toronto, Ontario, Canada M5S 1A7*

(Received 13 July 1990)

We construct a symmetry-based, competing-interaction model for the phase-transition sequence in betaine calcium chloride dihydrate (BCCD). Our model qualitatively reproduces experimentally observed behavior including the wave-vector sequence and the polarization properties. In addition, the model predicts space-group symmetries for the modulated phases.

The dielectric anomalies discovered by Rother *et al.*<sup>1</sup> in the crystal betaine calcium chloride dihydrate (BCCD) brought to light a particularly interesting sequence of structural phase transitions to modulated phases characterized, at least partially, by their modulation wave vectors. The modulation wave vectors  $k = \alpha(T)c^*$  (where  $c^* = 2\pi/c$ ) of the most prominent of the modulated phases have been directly determined by x-ray diffraction by Brill and Ehses.<sup>2</sup> They found that between the normal-incommensurate transition temperature of 164 K and the temperature 127 K the modulation is incommensurate (INC) with  $\alpha(T)$  varying from 0.32 to 0.285. Between 127 and 125 K a commensurate phase occurs with  $\alpha = \frac{2}{7}$ . Between 125 and 116 K, there is a further continuous change of wave vector ( $0.285 > \alpha > 0.25$ ), and below 116 K phases with  $\alpha = \frac{1}{4}$  ( $116 > T > 73$  K),  $\alpha = \frac{1}{5}$  ( $73 > T > 47$  K), and  $\alpha = \frac{1}{6}$  ( $47$  K  $> T$ ) occur. The recent EPR result by Ribeiro *et al.*,<sup>3</sup> however, suggests that the low-temperature phase (say  $T < 46$  K) of BCCD is unmodulated corresponding to  $\alpha = 0$ .

Between the phases just mentioned, a variety of higher-order commensurate phases appear in experiments. For example, Perez-Mato<sup>4</sup> had suggested, on the basis of the dielectric properties of BCCD, that three additional phases that are polar in the  $b$  direction and that would be likely to have  $\alpha$  values of  $\frac{4}{15}$ ,  $\frac{2}{9}$ , and  $\frac{2}{11}$  occur at temperatures of about 116, 75, and 56 K, respectively. These three phases have been confirmed by pyroelectric and dielectric measurements by Ribeiro *et al.*<sup>5-7</sup> Still high-order commensurate phases have been discovered by Unruh, Hero, and Drořák<sup>8</sup> using dielectric and thermal measurement, and by Ao and co-workers<sup>9</sup> using pressure-dependent dielectric measurements.

Symmetry arguments,<sup>4,8</sup> combined with the experimentally determined polar properties of the observed phases, have been used to assign  $\alpha$  values to these phases for which the  $\alpha$  values have not been measured directly. Perez-Mato's<sup>4</sup> argument starts from an analysis of the diffraction pattern of the incommensurate phases, from which he determines both the incommensurate phase superspace group and the phonon mode responsible for the normal-incommensurate transition; this mode has  $k = \alpha c^*$  and  $\Lambda_3$  symmetry, i.e., little co-group characters  $\chi(E) = \chi(\sigma_x) = 1$  and  $\chi(C_{2z}) = \chi(\sigma_y) = -1$ . Possible space-group symmetries for the commensurate phases are

also determined by Perez-Mato. The dielectric measurements and interpretation in the article by Unruh *et al.* also point to an order parameter of  $\Lambda_3$  symmetry (in Perez-Mato's notation) for the normal-incommensurate transition.<sup>8</sup>

A successful theoretical model for the modulated phases in BCCD must account for the modulation wave-vector sequence, the space-group symmetries, and the polar properties of the different phases. A number of authors have pointed out that the wave-vector sequence of the different phases in BCCD is of the "devil's staircase" type produced by competing-interaction models such as the axial next-nearest-neighbor Ising (ANNNI) model<sup>10</sup> and the Janssen-Tjon model.<sup>11</sup> Unfortunately, the relationship of the basic variables of these models (e.g., the spin variables of the ANNNI model) to physical variables appropriate to the BCCD system is either nonexistent or obscure, and predictions of space-group symmetries and polar properties for BCCD have not been made in terms of such models.

Landau theories are capable of predicting symmetries and polar properties of modulated phases, and some progress has been made in elucidating these properties in BCCD in terms of Landau theoretical ideas.<sup>4,8,12</sup> In a conventional Landau theory, however, a different lock-in term is required to stabilize each distinct commensurate wave vector, and a universal theory describing the full sequence of phase transitions that occurs in BCCD would require a large number of independent lock-in terms. An initial step in this direction was recently made by Ribeiro *et al.*<sup>13</sup> who chose the magnitude of four distinct lock-in contributions to the free energy in such a way as to stabilize the four most prominent commensurate phases of BCCD in appropriate temperature intervals without, however, attempting to predict the symmetries of these phases.

The challenge is thus to establish a single theoretical model that accounts for the physical properties of the sequence of modulated structure observed in BCCD. Recently, Chen and Walker<sup>14</sup> constructed a model that successfully described the structural properties of the various modulated structures occurring in the sequences of phase transitions found in the  $A_2BX_4$  family<sup>15</sup> (of which  $K_2SeO_4$  is the prototypical example). Here, we show that a similar approach is successful in the case of BCCD also.

The normal-phase structure of BCCD is orthorhombic (space group  $Pnma$ ) with four formula units  $[(\text{CH}_3)_3\text{NCH}_2\text{COO}\cdot\text{CaCl}_2\cdot 2\text{H}_2\text{O}]$  in the unit cell. Details of the structure can be found in the article by Brill, Schildkamp, and Spilker<sup>16</sup> For our purposes, rather than following the motions of all the ions in the unit cell during the successive phase transitions, it will be sufficient to following the motions of only the four nitrogen ions, or equivalently, of the four calcium ions. The four nitrogen ions in the unit cell can be associated with planes at  $z=c/4$  and  $3c/4$  (two ions to each plane) through the unit cell as shown in Fig. 1. Furthermore, it will be convenient to consider all of the ions in unit cell as being associated with one or other of the planes at  $z=c/4$  and  $3c/4$ . For example the betaine unit  $(\text{CH}_3)_3\text{NCH}_2\text{COO}$  associated with each nitrogen is associated with the plane to which the nitrogen belongs. Similarly, the  $\text{CaCl}_2\cdot 2\text{H}_2\text{O}$  unit associated with each calcium ion is associated with the plane to which the calcium ion belongs.

It was noted above that the three-dimensional symmetry mode, which is responsible for the phase transition from the normal high-temperature structure to the modulated structure, has wave vector  $k=ac^*$  and is of  $\Lambda_3$  symmetry.<sup>4</sup> Our approach is to develop a competing-interaction type of model that will necessarily be based on local variables. To achieve this end we consider BCCD to be made up of layers oriented normal to the  $c$  axis as described in the preceding paragraph and analyze the symmetry modes of the individual layers. The appropriate local variables of our theory will be those layer modes that can be used to make up three-dimensional modes with wave vectors  $k=ac^*$  and  $\Lambda_3$  symmetry.

To characterize a symmetry mode of a layer it is sufficient to give only the displacements that the nitrogen ions have in that mode. The other ions in the layer move also, in a given mode, but in a way that is determined once the displacements of the nitrogen ions are given. Since we will ultimately consider structures that are modulated in the  $c$  direction, but not in the  $a$  or  $b$  direc-

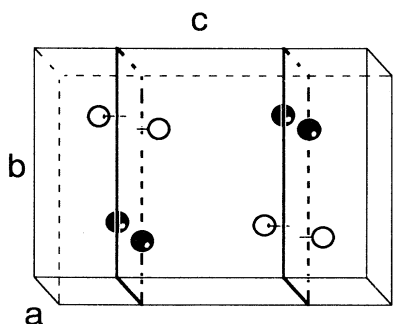


FIG. 1. The structure of BCCD at its normal phase. Each unit cell contains four formula units. The four nitrogen ions (open circles) and the four calcium ions (solid circles) are shown explicitly in this figure to characterize the symmetry. The betaine units are attached to the N ions, and the  $\text{CaCl}_2\cdot 2\text{H}_2\text{O}$  units are attached to the Ca ions (compare with Fig. 4 in Ref. 16).

tions, it is necessary to consider only those symmetry modes of a layer for which the relative ion motions in the layer unit cell are the same for all layer unit cells in that layer. The relevant layer symmetry modes are called here the  $\Gamma_2$  and  $\Gamma_3$  modes and are shown in Figs. 2 and 3. These modes can be represented more formally in terms of the vectors

$$e_l(\Gamma_2)=(1, -1), \quad e_l(\Gamma_3)=(1, 1). \quad (1)$$

Here the first and second entries describe the displacements in the  $b$  direction for ion (2) and ion (4) for odd  $l$ , and for ion (1) and (3) for even  $l$  (here  $l$  is an integer labeling the layer). The transformation properties of the symmetry-mode eigenvectors under the generators of the  $Pnma$  space group of the BCCD structure can be shown, from inspection of Figs. 2 and 3, to be

$$\begin{aligned} \{\sigma_x | \frac{1}{2} \frac{1}{2} \frac{1}{2}\} e_l(\Gamma_j) &= e_{l+1}(\Gamma_j), \\ \{\sigma_y | 0 \frac{1}{2} 0\} e_l(\Gamma_j) &= -e_l(\Gamma_j), \\ \{\sigma_z | \frac{1}{2} 0 \frac{1}{2}\} e_l(\Gamma_j) &= \pm e_{-l}(\Gamma_j), \end{aligned} \quad (2)$$

where  $j=2,3$  and the minus (or plus) sign in the third equation goes with  $\Gamma_2$  (or  $\Gamma_3$ ). The last two of these equations, for  $l=0$ , generate the characters of the  $\Gamma_2$  (or  $\Gamma_3$ ) representation for a single layer.

The Bloch states corresponding to the layer modes  $\Gamma_j$  are

$$e_k^j = \sum_l \exp(ikz_l) e_l(\Gamma_j), \quad (3)$$

where  $z_l=lc'$ , and  $c'=c/2$  is the interlayer distance. By making use of Eqs. (3), one can show that  $e_k^j$  (for  $j=2,3$ ) is a mode of  $\Lambda_3$  symmetry as defined above provided  $0 < |k| < \pi/(2c')$ . [For  $\pi/(2c') < |k| < \pi/c'$ ,  $e_k^j$  transforms as a  $\Lambda_2$  mode with characters  $\chi(E)=\chi(C_{2z})=1$ ,  $\chi(\sigma_x)=\chi(\sigma_y)=-1$ .] Furthermore, the other single-layer modes not considered above, which may be called the  $\Gamma_1$  and  $\Gamma_4$  modes, give three-dimensional modes of  $\Lambda_1$  and  $\Lambda_4$  symmetry (in Perez-Mato's notation) and therefore need not be considered.

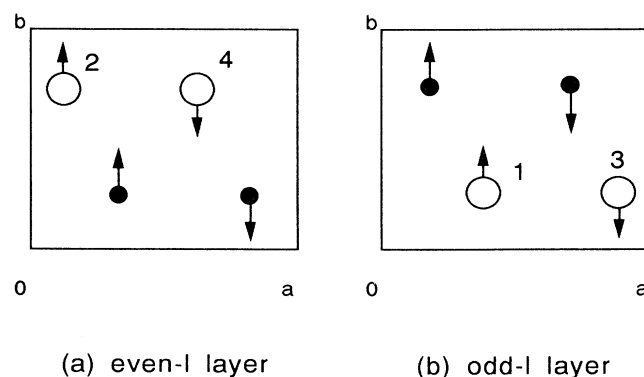


FIG. 2. The nitrogen-ion displacements in the single-layer modes of  $\Gamma_2$  symmetry for (a) even- $l$  layers and (b) odd- $l$  layers.

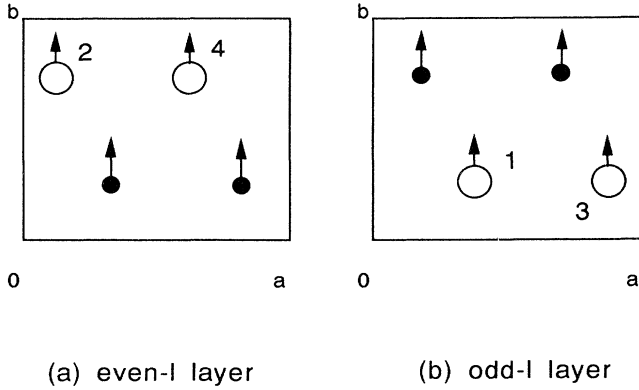


FIG. 3. The nitrogen-ion displacements in the single-layer modes of  $\Gamma_3$  symmetry for (a) even- $l$  layers and (b) odd- $l$  layers.

The displacement of ions in layer  $l$  are thus represented by the vector

$$u_l = v_l e_l(\Gamma_2) + w_l e_l(\Gamma_3). \quad (4)$$

The free energy, which is invariant under the transformations of the space group  $Pnma$ , can be written as

$$F_0 = \sum_n \left( \frac{1}{2} a v_l^2 + \frac{1}{4} v_l^4 + \frac{1}{2} a' w_l^2 + \frac{1}{4} w_l^4 + \frac{1}{2} b v_l^2 w_l^2 \right) + \frac{1}{2} \sum_l (J v_l v_{l+1} + J' w_l w_{l+1}) + \frac{1}{2} \sum_l (v_l w_{l+1} - v_{l+1} w_l). \quad (5)$$

There are five independent parameters in Eq. (3),  $a_{\pm} = \frac{1}{2}(a \pm a')$ ,  $J_{\pm} = \frac{1}{2}(J \pm J')$ , and  $b$ .

This free energy of Eq. (5) is identical to that used by the authors in Ref. 14 to describe the modulated structures found in the  $A_2BX_4$  family. We therefore refer to Ref. 14 for a discussion of the details of minimizing this free energy. Different classes of behavior, differing, for example, in the space-group symmetries assigned to phases of different wave vectors, can be obtained depending on the numerical values chosen for the parameters appearing in the free energy. In this article we fix  $a_- = 0.4$ ,  $J_- = 0$ , and  $b = 3$ , and allow  $a_+$  and  $J_+$  to vary, thus producing the phase diagram shown in Fig. 4. This choice of parameters produces a phase diagram that accurately describes the structural properties of BCCD. There is a range of parameters around the chosen values for  $a_-$ ,  $J_-$ , and  $b$  that would do equally well, and no claim is made that the particular set of parameters chosen is the best.

The different phases in Fig. 4 are labeled by the quantity  $\alpha$  in the relation  $k = \alpha c^*$ . Only commensurate phases were investigated, and for these we took  $\alpha = 2n/m$  (the 2 in the numerator occurs because the unit cell has two layers; also, the ratio  $n/m$  is assumed to be irreducible). Phases corresponding to all rational ratios  $n/m \leq 1/2$  with  $m$  from 1 to 15 were considered, and the phase diagram of Fig. 4 gives the results indicating which phase

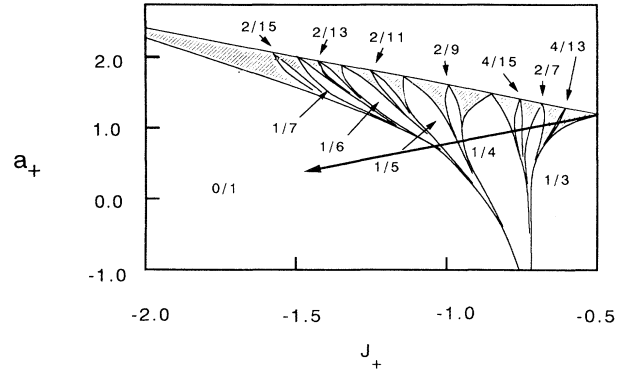


FIG. 4. The phase diagram produced from our model with  $\gamma = 3$ ,  $a_- = 0.4$ , and  $J_- = 0$ . The commensurate phases are represented by  $2n/m$ , where  $(2n/m)c^*$  is the wave vector and where the integer  $m$  is taken from 1 to 15. The shaded areas represent high-order commensurate and/or incommensurate regions. A possible trajectory of the sequence of the phases in BCCD at ambient pressure is also shown.

has the lowest free energy at the stated values of the parameters. The shaded areas indicate higher-order commensurate and/or incommensurate regions.

The parameters in our model are assumed to be temperature and pressure dependent. Changing the temperature at ambient pressure for BCCD will therefore correspond to our phase diagram following a particular trajectory in the model parameter space. A trajectory giving the sequence of phase transitions observed in BCCD is shown in Fig. 4, where it can be seen that, as the temperature is lowered,  $\alpha$  follows the sequence of modulation wave vectors  $\alpha = \text{INC}, \frac{4}{13}, \text{INC}, \frac{2}{7}, \text{INC}, \frac{4}{15}, \frac{1}{4}, \frac{2}{9}, \frac{1}{5}, \frac{2}{11}, \frac{1}{6}$ , and 0. Also, the relative sizes of the temperature intervals over which the various phases are stable correspond approximately to the relative sizes of the corresponding intervals in Fig. 4.

The pressure-temperature phase diagram of BCCD, reported by Ao and co-workers from a dielectric constant measurement,<sup>9</sup> qualitatively agrees with Fig. 4 if we assume that the variables  $a_+$  and  $J_+$  are temperature and pressure dependent. The phase diagram of Ao and co-workers also contains some high-order commensurate phases; since we only took  $m \leq 15$  in Fig. 4, these high-order commensurate phases are not explicitly shown in Fig. 4 (see, however, Fig. 6 for an exploded phase sequence).

The space-group symmetry for each commensurate phase can be found from the numerically determined profile of  $v_l$  and  $w_l$  as in Ref. 14. In particular, our model predicts the space-group symmetries  $Pn2_1a$  for wave vectors  $\alpha = \text{even-odd}$ ,  $P2_12_12_1$  for  $\alpha = \text{odd-odd}$ ,  $P2_1ca$  for  $\alpha = \text{odd-even}$ , and the superspace-group symmetry  $P_{151}^{Pnma}$  for the incommensurate phases. These results are in agreement with those deduced by Perez-Mato<sup>4</sup> (by combining symmetry arguments with the results of polarization measurements) for the cases  $\alpha = \text{even-odd}$  and  $\alpha = \text{odd-even}$ . For the case  $\alpha = \text{odd-odd}$ , Perez-Mato arrives at two possible space groups, one of these being the

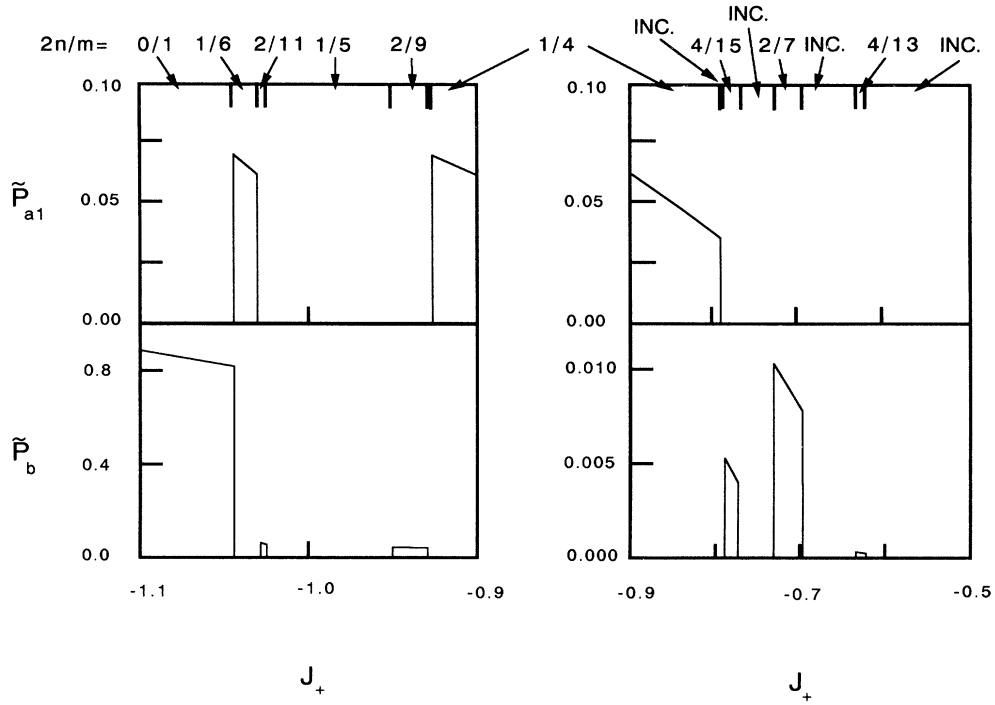


FIG. 5. Spontaneous polarization calculated from our model, where commensurate phases with  $m$  values from 1 to 15 are considered. The value of  $J_+$  shown here labels a point on the trajectory  $a_+ = 0.8J_+ + 1.6$ , as shown in Fig. 4.

one predicted by our model.

To further compare the results of our model with experimental measurements of the polarization properties in BCCD, we have calculated the polarization from our model. To do this we consider the polarization to be a function of the variables  $v_l$  and  $w_l$ . Expanding  $P_b$  in powers of the  $v_l$  and  $w_l$  and keeping only terms consistent with the symmetry  $Pnma$  of the normal phase, we find that  $P_b$ , to first order in these variables, can be written as

$$P_y = c_b - \sum_l w_l \equiv c_b \tilde{P}_y. \quad (6)$$

The polarization  $P_a$  has no contribution linear in  $v_l$  or  $w_l$ . To second order, and including only products in which both variables are associated either with the same layer or neighboring layers, we find that  $P_a$  can be written  $P_a = P_{a1} + P_{a2} + P_{a3}$  with

$$\begin{aligned} P_{a1} &= c_{a1} - \sum_l (-1)^l v_l (w_{l+1} - w_{l-1}) \equiv c_{a1} \tilde{P}_{a1}, \\ P_{a2} &= c_{a2} - \sum_l (-1)^l v_l^2 \equiv c_{a2} \tilde{P}_{a2}, \\ P_{a3} &= c_{a3} - \sum_l (-1)^l w_l^2 \equiv c_{a3} \tilde{P}_{a3}. \end{aligned} \quad (7)$$

In Fig. 5, the quantities  $\tilde{P}_{a1}$  and  $\tilde{P}_b$  are plotted as functions of  $J_+$  along the trajectory  $a_+ = 0.8J_+ + 1.6$  shown in Fig. 4. The orders of magnitude of the quantities  $\tilde{P}_{a2}$  and  $\tilde{P}_{a3}$  are the same as that of  $\tilde{P}_{a1}$ ; these two quantities therefore are not shown in Fig. 5. The calculated relative magnitudes of the polarization in the different phases,

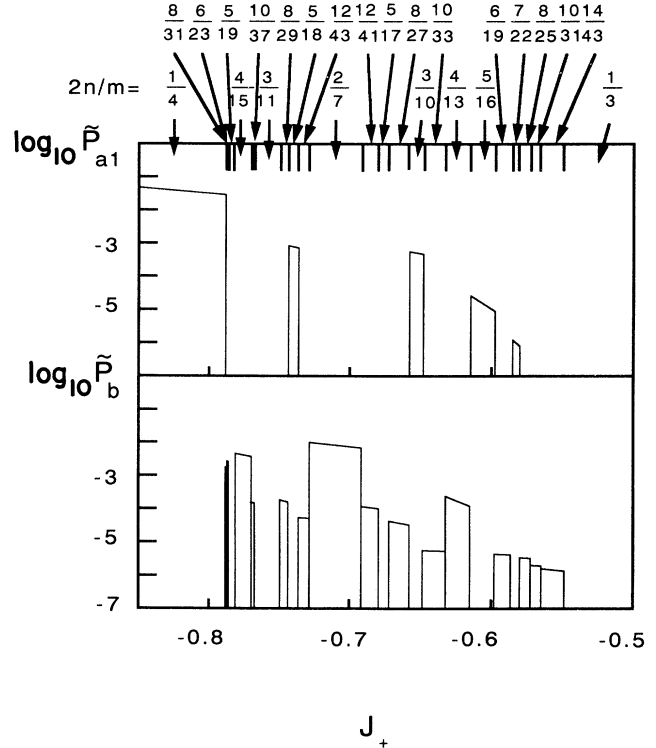


FIG. 6. Spontaneous polarization calculated from our model for  $J_+ = -0.5$  to  $-0.85$  where commensurate phases with  $m$  values from 1 to 45 are considered. As in Fig. 5,  $J_+$  labels points on the trajectory shown in Fig. 4.

and the calculated relative widths of the temperature (or  $J_+$ ) intervals over which these phases are stable are in striking agreement with the corresponding quantities measured experimentally by Ribeiro *et al.*<sup>6,7</sup> This is so for the phases corresponding to  $\alpha = \text{INC}, \frac{2}{7}, \text{INC}, \frac{4}{15}, \frac{1}{4}, \frac{2}{9}, \frac{1}{5}, \frac{2}{11}, \frac{1}{6}$ , and 0.

In Fig. 6, an expanded view of the interval from  $J_+ = -0.5$  to  $-0.85$  is shown. All of the additional phases seen by Unruh, Hero, and Drořák<sup>8</sup> in this interval (e.g.,  $\alpha = \frac{3}{10}, \frac{5}{18}, \frac{3}{11}$ , and  $\frac{6}{23}$ ) are found in this figure with exception of the phase for which  $\alpha = \frac{7}{26}$ . The reason a phase corresponding to  $\alpha = \frac{7}{26}$  is missing from our figure is that our calculations went up to  $m = 45$  only (recall  $\alpha = 2n/m$ ) and  $\alpha = \frac{7}{26}$  corresponds to  $m = 52$ . A number of the phases shown in Fig. 6 have not been observed experimentally. The predicted magnitudes of the polarizations of the unobserved phases are, however, much smaller than those of the observed phases (note the logarithmic

scale in Fig. 6).

As a final point, note that the phases labeled  $\alpha = \frac{1}{8}$  and  $\frac{1}{7}$  by Unruh, Hero, and Drořák<sup>8</sup> do not appear in Fig. 5 because of the special trajectory used. It is clear from Fig. 4, however, that if we had raised the most negative  $J_+$  end of our chosen trajectory slightly, we would have obtained these phases also.

In conclusion, we note that the symmetry-based competing-interaction model developed in this article to describe the various modulated structures occurring in BCCD gives a remarkably detailed account of all of the observed phases and their polarization properties. Phases other than those observed are also predicted by the analysis, but have much smaller polarizations than those of the phases already observed.

*Note added in proof:* Several relevant papers<sup>17–20</sup> were overlooked in the initial preparation of this manuscript.

\*Present address: Xerox Research Centre of Canada, 2660 Speakman Drive, Mississauga, Ontario, Canada, L5K 2L1.

<sup>1</sup>H. J. Rother, J. Albers, and A. Klöpperpieper, *Ferroelectrics* **54**, 107 (1984).

<sup>2</sup>W. Brill and K. H. Eshes, *Jpn. J. Appl. Phys.* **24**, Suppl. 24-2, 826 (1985).

<sup>3</sup>J. L. Ribeiro, J. C. Fayet, J. Emery, M. Pézeril, J. Albers, A. Klöpperpieper, A. Almeida, and M. R. Chaves, *J. Phys. (Paris)* **49**, 813 (1988).

<sup>4</sup>M. Perez-Mato, *Solid State Commun.* **67**, 1145 (1988).

<sup>5</sup>J. L. Ribeiro, M. R. Chaves, A. Almeida, J. Albers, A. Klöpperpieper, and H. E. Mueser, *J. Phys. Condens. Matter* **1**, 8011 (1989).

<sup>6</sup>J. L. Ribeiro, M. R. Chaves, A. Almeida, J. Albers, A. Klöpperpieper, and H. E. Müser, *Phys. Rev. B* **39**, 12 320 (1989).

<sup>7</sup>J. L. Ribeiro, M. R. Chaves, A. Almeida, J. Albers, and A. Klöpperpieper, and H. E. Müser, *Ferroelectrics Lett.* **8**, 135 (1988).

<sup>8</sup>H. G. Unruh, F. Hero, and V. Drořák, *Solid State Commun.* **70**, 403 (1989).

<sup>9</sup>R. Ao, G. Schaack, M. Schmitt, and M. Zöller, *Phys. Rev. Lett.* **62**, 183 (1989); R. Ao and G. Schaack, *Indian J. Pure*

*Appl. Phys.* **26**, 124 (1988).

<sup>10</sup>P. Bak and J. von Boem, *Phys. Rev. B* **21**, 5297 (1980); for a recent review, see W. Selke, *Phys. Rep.* **170**, 213 (1988).

<sup>11</sup>T. Janssen and J. A. Tjon, *Phys. Rev. B* **24**, 2245 (1981); **25**, 3767 (1982).

<sup>12</sup>V. Drořák, J. Holakovský, and J. Petzelt, *Ferroelectrics* **79**, 15 (1988).

<sup>13</sup>J. L. Ribeiro, J. C. Tolédano, M. R. Chaves, A. Almeida, H. E. Müser, J. Albers, and A. Klöpperpieper, *Phys. Rev. B* **41**, 2343 (1990).

<sup>14</sup>Z. Y. Chen and M. B. Walker, *Phys. Rev. Lett.* **65**, 1223 (1990).

<sup>15</sup>R. Blinc and A. P. Levanyuk, *Incommensurate Phases in Dielectrics* (North-Holland, Amsterdam, 1986); H. Z. Cummins, *Phys. Rep.* **185**, 211 (1990).

<sup>16</sup>W. Brill, W. Schildkamp, and J. Spilker, *Z. Kristallogr.* **172**, 281 (1985).

<sup>17</sup>T. Tentrup and R. Siems, *Ferroelectrics* **98**, 303 (1989); R. Siems and T. Tentrup, *ibid.* **105**, 379 (1990).

<sup>18</sup>R. Currat, J. F. Legrand, S. Kamba, J. Petzelt, V. Drořák, and J. Albers, *Solid State Commun.* **75**, 545 (1990).

<sup>19</sup>V. Drořák, *Ferroelectrics* **104**, 135 (1990).

<sup>20</sup>G. Schaack, *Ferroelectrics* **104**, 147 (1990).